Application of Stochastic Robustness to Aircraft Control Systems

Laura Ryan Ray* and Robert F. Stengel†
Princeton University, Princeton, New Jersey 08544

Stochastic robustness, a simple numerical procedure for estimating the stability effects of parameter uncertainty in linear, time-invariant systems, is applied to a forward-swept-wing aircraft control system. Based on Monte Carlo evaluation of the system's closed-loop eigenvalues, this analysis approach introduces the probability of instability as a scalar stability robustness measure. The related stochastic root locus provides insight into modal variations of the closed-loop system. Three linear-quadratic optimal controllers are chosen to demonstrate the use of stochastic robustness to analyze and compare control designs. The example considers the stability robustness effects of uncertain actuator dynamics and higher order dynamics. Analysis of stochastic robustness is shown to provide a valuable tool for control system design.

Introduction

CONTROL system robustness is the ability to maintain satisfactory stability and/or performance characteristics in the presence of all conceivable system parameter variations. While assured robustness may be viewed as an alternative to gain adaptation or scheduling to accommodate known parameter variations, more often it is seen as protection against uncertainties in plant specification. Consequently, a statistical description of control system robustness is consistent with what may be known about the structure and parameters of the plant's dynamic model.

Guaranteeing robustness has long been a design objective of control system analysis, although in most instances, insensitivity to parameter variations has been treated as a deterministic problem (see Ref. 1 for a comprehensive presentation of both classical and modern robust control). The probability of instability, which is central to stochastic robustness analysis, was introduced in Ref. 2, with application to the robustness of the Space Shuttle's flight control system, and it is further described in Ref. 3. This method determines the stochastic robustness of a linear, time-invariant system by the probability distributions of closed-loop eigenvalues, given the statistics of the variable parameters in the plant's dynamic model. The probability that all of these eigenvalues lie in the open-left-half s plane is the scalar measure of robustness. The stochastic robustness of a system is easily computed by Monte Carlo simulation, and results can be displayed pictorially, providing insight into otherwise hidden robustness properties of the system. The method is computationally simple, requiring only matrix manipulation and eigenvalue computation, and it is inherently nonconservative, given a large enough number of Monte Carlo evaluations. Confidence intervals for the probability of instability are readily computed. References 4–6 describe in detail the application of stochastic robustness and the related probability of instability and stochastic root locus, which are briefly summarized here.

Received July 10, 1989; revision received Nov. 14, 1990; accepted for publication Nov. 20, 1990.

*Graduate Student, Department of Mechanical and Aerospace Engineering; currently, Assistant Professor, Department of Mechanical Engineering, Clemson University, Clemson, SC.

†Professor, Department of Mechanical and Aerospace Engineering. Associate Fellow AIAA.

Probability of Instability

Consider a linear, time-invariant (LTI) system subject to LTI control:

$$\dot{x}(t) = F(p)x(t) + G(p)u(t) \tag{1}$$

$$y(t) = H(p)x(t) \tag{2}$$

$$u(t) = u_c(t) - CH(p)x(t) \tag{3}$$

where $x(t)$, $u(t)$, $y(t)$, and p are state, control, output, and parameter vectors of dimension n, m, q, and r, respectively. They are accompanied by conformable dynamic, control, and output matrices F, G, and H, whose elements may be arbitrary functions of p; $u_c(t)$ is a command input vector, and for simplicity, the $(m \times n)$ control gain matrix C is assumed to be known without error. The n eigenvalues, $\lambda_i = \sigma_i + j\omega_i$, $i = 1, \ldots, n$, of the matrix $[F(p) - G(p)CH(p)]$ determine closed-loop stability. Whereas the explicit relationship between parameters and eigenvalues is complicated, estimating the probability of instability of the closed-loop system from repeated eigenvalue calculation is a straightforward task.[4-6] Denoting the probability density function of p as $pr(p)$, the closed-loop eigenvalues are evaluated J times with each element of $p_j (j = 1, \ldots, J)$ specified by a random-number generator whose individual outputs are shaped by $pr(p)$. This Monte Carlo evaluation of the probability of instability becomes increasingly precise as J becomes large.

Stochastic robustness is achieved when the probability of instability P is small. Since stability requires all the roots to be in the open-left-half s plane, and the probability of stability plus the probability of instability is one, we may write

$$Pr(\text{instability}) \triangleq P = 1 - \int_{-\infty}^{0} pr(\sigma)\, d\sigma \tag{4}$$

$$= 1 - \lim_{J \to \infty} \frac{N(\sigma_{\max} \leq 0)}{J} \tag{5}$$

where σ is an n vector of the real parts of the system's eigenvalues, and $pr(\sigma)$ is the joint probability density function of σ. The integral that defines the probability of stability is evaluated over the space of individual components of σ. $N(\cdot)$ is the number of cases for which all elements of σ are less than or equal to zero, that is, for which $\sigma_{\max} \leq 0$, where $\sigma_{\max}$ is the maximum real eigenvalue component in σ. This definition does not depend on the eigenvalues and eigenvectors retaining fixed structures. As parameters, change, complex roots may coalesce to become real roots (or the reverse), and modes may

exchange relative frequencies. The only matter for concern is whether or not all real parts of the eigenvalues remain in the left-half s plane. For $J < \infty$, the computed probability of instability resulting from Monte Carlo evaluation is an estimate, denoted $\hat{P}$.

Gaussian, uniform, Rayleigh, correlated, and any other well-posed distributions are admissible specifications for the multivariate $pr(p)$, the principal challenge being to properly shape (and correlate) the outputs of the random-number generator. In practice, system parameter uncertainties are most likely to be bounded, as typical quality control procedures eliminate out-of-tolerance devices, and there are physical limitations on component size, weight, shape, etc. The rectangular (uniform) distribution is particularly interesting, as it readily models bounded uncertainty, and it is the default distribution of most random-number generators. Given binary distributions for each parameter, in which the elements of p take maximum or minimum values with equal probability, the Monte Carlo evalution reduces to 2^r deterministic evaluations, the result is exact, and the probability associated with each possible value of p is $\frac{1}{2}^r$. For parameters quantized at w levels, w^r evaluations provide an exact measure of the probability of instability.

Stochastic Root Locus

Stochastic root loci[4-6] provide insight regarding the effects of parameter uncertainty on system stability. Root loci for individual parameter variations follow classical configurations of root locus construction,[7] with the heaviest density of roots in the vicinities of the nominal roots. The density of roots resulting from Monte Carlo analysis, or the stochastic root locus, depicts the likelihood that eigenvalues vary from their nominal values if combinations of parameters are uncertain. Stochastic root loci can include branches on the real axis and in the right-half s plane for large enough parameter variations.

Understanding of robustness issues can be gained by plotting the density of the roots in a third dimension above the root locus plot. One method of doing this is simply to divide the s plane into subspaces (or bins), and to count the number of roots in each bin as a sampled estimate of the root density ρ. The result is a multivariate histogram, with σ and ω serving as independent variables. Complex root bins are elemental areas, for which the density is defined in units of roots/unit area. Real root bins are confined to the real axis; hence, the root density measures roots/unit length. The stochastic root loci can be portrayed by graphing contours of equal root density on a two-dimensional plot or by plotting an oblique view of the three-dimensional histogram or root density surface.

Confidence Intervals

Associated with the estimate $\hat{P}$ are confidence intervals that bound the (unknown) true underlying probability of instability P with defined certainty. A confidence statement for P is

$$Pr(L < P < U) = 1 - \alpha \tag{6}$$

where (L,U) is the interval estimate (lower and upper bounds), and $1-\alpha$ is the confidence coefficient. Equation (6) states that P lies within (L,U) with $100(1-\alpha)\%$ confidence. The probability of instability is a binomial variable, with the outcome of each Monte Carlo trial taking one of two possible values (stable or unstable). Confidence intervals for probability of instability are based on the binomial test[8] and are detailed in Refs. 5 and 6.

The number of evaluations required for a desired confidence interval width is an important practical aspect of stochastic robustness analysis. Figure 1 (from Ref. 6) presents the number of evaluations required for specified interval widths and a 95% confidence coefficient, given as a percentage of P. An estimate of $\hat{P}$ based on a small number of evaluations can be used as the abscissa of Fig. 1 to forecast the total number of evaluations required for the desired interval width. For very narrow intervals and small probabilities of instability, large numbers of evaluations are required. However, for small P, large interval widths as a percent of P are acceptable. For instance, when $P = 10^{-6}$, an interval width of 100% P or 10^{-6} gives an interval estimate $(L,U) = (5.72E\text{-}7,\ 1.572E\text{-}6)$. (The asymmetry around P results from application of the binomial test.) A larger confidence coefficient shifts the curves of Fig. 1 to higher numbers of evaluations.

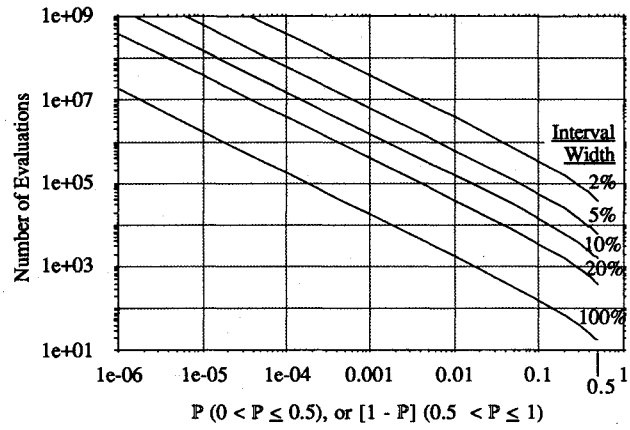

Fig. 1 Number of evaluations required for given confidence interval widths and confidence coefficient $1-\alpha = 0.95$. Interval width is given as percent of P or $1-P$.

The validity of Monte Carlo analysis depends on a number of simulation parameters: the number of system eigenvalues, the number of uncertain parameters, and parameter probability distributions. By applying binomial confidence intervals, the derivation of explicit relationships between simulation parameters and the required number of evaluations is avoided. Nevertheless, the binomial test offers a rigorous theory by which to calculate exact confidence intervals. The number of evaluations required for a given interval width can be related to a single variable P, and the relationship is valid for any combination of simulation parameters and any application.

Characteristics of the Analysis

Stochastic robustness analysis offers a logical alternative to traditional robustness measures, such as singular-value analysis. Unstructured-singular-value (USV) analysis[9] is restricted to systems with unstructured uncertainties; conservative robustness estimates can result when it is applied to systems with structured uncertainty. Furthermore, it is difficult to measure improvement between controller designs when the robustness measure is conservative. A less conservative measure results when structured-singular-value (SSV) analysis is applied,[10] but it is difficult to put known uncertainties, such as arbitrary parameter variations, into the form required for SSV analysis. (See Ref. 11 for a good discussion about modeling of uncertainties.) When applying either USV or SSV analysis, uncertainty magnitudes may not be easily related to physical parameters. Stochastic robustness requires that the uncertainty be described using parameters and their associated statistics. Hence the designer has the ability to identify parameters that greatly influence robustness. The scalar probability of instability is a direct measure of robustness improvement or degradation between controller designs. Parameter uncertainties must be associated with probability distributions for stochastic robustness analysis; bounded uniform distributions are analogous to the assumptions made in singular-value analysis. One might object that the parameter distributions must be known or estimated for stochastic robustness analysis. However, if robustness estimates are strongly dependent on the statistics, then it is incumbent on the designer to know something about them.

Finite-dimensional model-order uncertainties can be cast into the structured form required for stochastic robustness analysis. Higher order state dynamics and elements are appended to the reduced-order, linear model, and appropriate uncertainties are assigned to the associated parameters. Analysis proceeds with the gains established using the reduced-order model. Often, certain parameters, such as characteristic frequencies associated with unmodeled dynamics, are well known, while others such as coupling terms, are not easily measured. Stochastic robustness provides an excellent framework for studying such problems, as will be demonstrated by an example. It answers the question, How much uncertainty is allowable while still maintaining a robust design? Effects of actuator dynamics can be studied using stochastic robustness in a similar manner.

Stochastic Robustness Applied to a Forward-Swept-Wing Aircraft

This example, based on the longitudinal dynamics and control of an open-loop-unstable aircraft was introduced in Ref. 6 to describe the expression of a real problem with physical parameter uncertainties. Three applications of stochastic robustness are demonstrated here by means of the example: evaluating and comparing different control system designs for stability robustness, studying the effects of uncertain actuator dynamics, and including higher order dynamics in the analysis.

Control System Design Evaluation

Longitudinal motions of a Forward-Swept-Wing Demonstrator Aircraft flying at a Mach number of 0.6 and an altitude of 15,000 ft are described by Eq. (1) with

$$F = \begin{bmatrix} -0.02 & -0.3 & -0.4 & -32.2 \\ -0.0001 & -1.2 & 1 & 0 \\ 0 & 18 & -0.6 & 0 \\ 0 & 0 & 1 & 0 \end{bmatrix} \tag{7}$$

$$G = \begin{bmatrix} -0.04 & 35 \\ 0 & 0 \\ 0.2 & -0.2 \\ 0 & 0 \end{bmatrix} \tag{8}$$

The state components represent forward velocity, angle of attack, pitch rate, and pitch angle. The principal control surfaces are the canard control surface and the thrust setting. Because the aircraft's aerodynamic center is forward of its center of mass, the model possesses a static instability, which is reflected by a positive eigenvalue of F; the complete set of eigenvalues is

$$\lambda_{1\text{-}4} = -0.0102 \pm 0.057j, \quad -5.15, \quad 3.35 \tag{9}$$

Table 1 Parameters for Forward-Swept-Wing Demonstrator Aircraft

1) $Q = \text{diag}(1,1,1,0)$ $R = \text{diag}(1,1)$
$\lambda_{1\text{-}4} = 35.0, -5.14, -3.32, -0.018$
$$C = \begin{bmatrix} 0.1714 & 130.2604 & 33.1648 & 0.3642 \\ 0.9842 & -11.3867 & -2.9680 & -1.1329 \end{bmatrix}$$

2) $Q = \text{diag}(1,1,1,0)$ $R = \text{diag}(1000,1000)$
$\lambda_{1\text{-}4} = -5.15, -3.36, -1.09, -0.019$
$$C = \begin{bmatrix} 0.0270 & 82.6589 & 20.9266 & -0.0638 \\ 0.0107 & -62.6225 & -16.2029 & -1.9018 \end{bmatrix}$$

3) $\lambda_{1\text{-}4} = -32.21, -5.15, -3.44, -0.014$
$$C = \begin{bmatrix} 0.1349 & 413.2944 & 104.6331 & -0.3191 \\ 0.0535 & -313.1124 & -81.0146 & -9.5089 \end{bmatrix}$$

Possible uncertainties in aerodynamic and thrust effects contribute 10 elements to the parameter vector (the remaining terms are kinematic, due to gravity, identically zero, or otherwise negligible). Dynamic pressure (air density and velocity) effects can be modeled as uniform parameters and included in the parameter vector to represent a range of flight condition variations around the nominal condition. In terms of the parameters, F and G are

$$F = \begin{bmatrix} \frac{-2gf_{11}}{V} & \frac{\rho V^2 f_{12}}{2} & \rho V f_{13} & -g \\ \frac{-45}{V^2} & \frac{\rho V f_{22}}{2} & 1 & 0 \\ 0 & \frac{\rho V^2 f_{32}}{2} & \rho V f_{33} & 0 \\ 0 & 0 & 1 & 0 \end{bmatrix} \tag{10}$$

$$G = \frac{\rho V^2}{2} \begin{bmatrix} g_{11} & g_{12} \\ 0 & 0 \\ g_{31} & g_{32} \\ 0 & 0 \end{bmatrix} \tag{11}$$

where f_{ij} and g_{ij} are matrix elements of F and G with dynamic pressure effects factored, ρ is the air density, and V is the velocity. Physically, f_{ij} and g_{ij} represent stability and control derivatives that might be estimated analytically, based on the aircraft design, or experimentally via wind-tunnel testing. The corresponding 12-element parameter vector is defined as

$$p = [\rho V f_{11} f_{12} f_{13} f_{22} f_{32} f_{33} g_{11} g_{12} g_{31} g_{32}]^T \tag{12}$$

Each element of Eqs. (10) and (11) is a relatively complex function of the parameters; it would be difficult to express this kind of parametric uncertainty in the form required for deterministic robustness analysis. Stochastic robustness analysis handles such complexity routinely.

Stochastic robustness analysis is demonstrated using three examples. Linear-quadratic optimal controllers have been designed (as in Ref. 3) according to three specifications: 1) $Q = \text{diag}(1,1,1,0)$, $R = \text{diag}(1,1)$; 2) $Q = \text{diag}(1,1,1,0)$, $R = \text{diag}(1000,1000)$; and 3) the control gain matrix of case 2 is multiplied by an arbitrary factor (5) to restore the closed-loop bandwidth to that of case 1. The resulting control gain matrices and corresponding nominal closed-loop eigenvalues are given in Table 1. These three cases have not been chosen to satisfy any particular performance criteria; they merely demonstrate the impact of differing generalized design criteria on stochastic robustness. Furthermore, the designs are not meant to reflect acceptable control laws, as the high gains were purposely chosen to magnify stability robustness problems and to illustrate the application of stochastic robustness. Based on the control weighting matrix (R) specifications and the ad hoc robustness recovery technique, the controllers were designed to increase in stability robustness from case 1 to case 3.

Comparison with Singular-Value Analysis

Before treating all parameter variations concurrently, consider the effects of two separate parameter variations on closed-loop stability, as well as the stability bounds predicted by singular-value analysis. The large positive value of f_{32} is the principal cause of the open-loop static instability, whereas g_{31} is the primary control effect for providing closed-loop stabil-

Table 2 Stability bounds predicted by singular-value analysis for single parameter variation in the Forward-Swept-Wing Demonstrator Aircraft

Case parameter	1	2	3	1	2	3
	f_{32} (nominally 0.05276)			g_{31} (nominally 5.86E-4)		
Actual value causing instability	0.104	0.127	0.894	2.91E-4	1.20E-4	2.05E-5
Value predicted by USV	0.05285	0.0554	0.0559	5.85E-4	4.26E-4	5.26E-4

ity. USV analysis gives the largest allowable uncertainty magnitude as a function of frequency. Because the uncertainty is structured, USV analysis produces conservative bounds on the allowable magnitude of the uncertainty. Table 2 demonstrates just how conservative these results can be by showing the actual parameter variations that produce instability, as well as the bounds predicted using USV analysis. The largest additive uncertainty allowed for each separate parameter variation is computed using[9]

$$\bar{\sigma}\left[\Delta A(j\omega)\right] < \underline{\sigma}\left[I_m + A(j\omega)\right] \tag{13}$$

where $\bar{\sigma}$ and $\underline{\sigma}$ denote the largest and smallest singular values, respectively, and $A(j\omega) = C(j\omega I_n - F)^{-1}G$ and $\Delta A(j\omega)$ represent the largest allowable additive uncertainty over all frequencies ω. SSV analysis of real parameter variations[12] involves computation of the real structured singular value $\mu_R[M(j\omega)]$ for all frequencies ω:

$$\mu_R\left[M(j\omega)\right] = \left\{\min_{\Delta \epsilon X_\infty}\left[\bar{\sigma}(\Delta) \mid \det\left(I + M(j\omega)\Delta\right) = 0\right]\right\}^{-1} \tag{14}$$

where $M(j\omega)$ represents the perturbation structure of the feedback system and its uncertainties, Δ is a real, block-diagonal perturbation matrix whose elements have magnitudes less than or equal to one, and X_∞ is the set of all block-diagonal matrices. SSV analysis correctly predicts the instability bounds for these two individual parameter variations, and determining the parameter value that causes instability from μ_R for single parameter variations is trivial. However, application of SSV analysis to the system described by Eqs. (10) and (11) would be difficult; there are multiple parameters appearing in one or more matrix terms, and the effect of parameter uncertainty on the system is not necessarily linear. It would be difficult to express the feedback system uncertainties in terms of a block-diagonal perturbation matrix Δ and the associated matrix $M(j\omega)$. Furthermore, algorithms for accurately computing μ_R are not yet available, and existing algorithms (for the complex structured singular value) would yield conservative results.

What would the probability of instability be if f_{32} and g_{31} were independently subject to uncertainty? For illustration, uniform uncertainties of $\pm 30\%$ are considered; these are representative of very loose manufacturing tolerances or preflight testing results. By inspection of the actual values causing instability (Table 2), P would be identically zero for uniform or binary distributions of this magnitude, while the 25,000-evaluation results for Gaussian distributions are shown in Table 3.

The presentation of results in Tables 2 and 3 are, of course, very different. Table 2 presents robustness in terms of parameter values causing instability. A designer must evaluate singular values against appropriate unstructured or structured uncertainties to determine whether the system is sufficiently robust in the face of actual uncertainties. Stochastic robustness, on the other hand, incorporates parameter uncertainties as part of the analysis, and the resulting measure is statistical. Structured singular values can be related to individual parameter variations, but the task ranges from difficult to impossible for cases involving many parameters and system matrices that are arbitrary functions of the parameters. Nevertheless, such relationships are necessary to properly evaluate robustness at the parameter level. In this context, stochastic robustness is a simple but powerful analysis tool.

Table 3 Probability of instability and 95% confidence intervals (L,U) for single parameter variation in the Forward-Swept-Wing Demonstrator Aircraft[a]

Case	$\hat{P}$ f_{32} variation	(L,U) g_{31} variation	$\hat{P}$	(L,U)
1	0.00072	(4.27E-4, 1.14E-3)	0.0465	(0.0424, 0.0506)
2	0	(0.0, 1.48E-4)	0.004	(3.26E-3, 4.86E-3)
3	0	(0.0, 1.48E-4)	3.6E-4	(1.25E-4, 5.95E-4)

[a] Based on 25,000 Monte Carlo evaluations and 30% standard-deviation Gaussian uncertainty.

Simultaneous Variations in Twelve Parameters

Next, we examine the stochastic root loci for the three controller designs. Results for simultaneous parameter variations were presented in Ref. 6 and are summarized here. It is assumed that the velocity and density vary uniformly within $\pm 30\%$ of their nominal values to represent flight condition variations and that each of the remaining elements of p is subject to an independent 30%-standard-deviation Gaussian uncertainty. Figure 2 shows the stochastic root loci, based on 25,000 Monte Carlo evaluations. The corresponding probability-of-instability estimates and 95% confidence intervals are 1) 0.0724 (0.0692, 0.0756), 2) 0.0205 (0.0187, 0.0222), and 3) 0.0076 (0.0065, 0.0086). Robustness improves from case 1 to 3 as control usage is restrained by high control weighting, and the ad hoc robustness recovery technique used in case 3 gives additional improvement. While 95% confidence intervals for cases 2 and 3 initially overlap (Fig. 3), 25,000 evaluations is more than sufficient to rank the three cases in order of robustness. If all 12 parameters are uniformly distributed in $[0.7p, 1.3p]$, the extent of the parameter and eigenvalue distributions decreases substantially, as shown in Fig. 4 for case 3. A comparison of Fig. 2c and Fig. 4 indicates the effects of Gaussian "tails" on the eigenvalue probability densities. The 25,000-evaluation probability-of-instability estimates and 95% confidence intervals for uniformly distributed parameters are 3.6E-4 (1.25E-4, 5.95E-4) for case 1 and zero (0, 1.48E-4) for the remaining two cases.

Figure 5 shows stochastic stability robustness as a function of the control weighting parameter v ($R = vI_2$). For the specified parameter statistics, the distinction in stability robustness vs the design parameter is apparent, and maximum robustness occurs between $v = 10^2$ and 10^4. That the minimum-control-energy case ($v \to \infty$) represents the least robust design would not be obvious using standard robustness analysis techniques. Possible interaction between root-locus branches, the fact that the open-loop system is unstable, and the uncertainty present in the dynamic matrix all make it difficult to predict the value of v that maximizes robustness based on analysis of the nominal system. The kind of results presented in Fig. 5 offer controller design insight and clearly show nonobvious robustness characteristics.

It is not possible to conduct comparable singular-value analyses for these 12-parameter cases. Because such variations are structured, unstructured-singular-value analysis would predict an allowable loop-gain variation without regard to the allocation of element variations in p; it would be difficult to relate this result to specific parameter variations, and the result would be quite conservative. Structured-singular-value analysis could identify less conservative stability boundaries if the allocation of parameter variations were known or postulated,

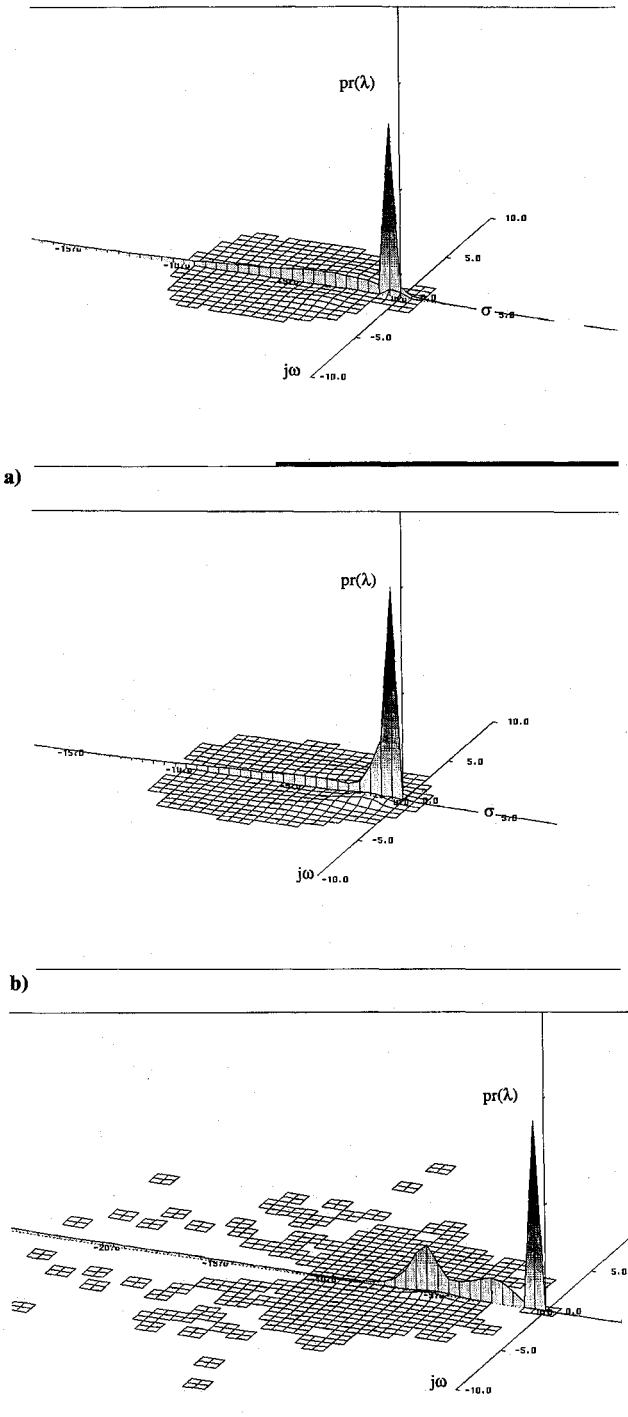

Fig. 2 Stochastic root loci for the Forward-Swept-Wing Demonstrator Aircraft with 30% Gaussian parameters, and ±30% uniform ρ, V, cases 1, 2, and 3. Based on 25,000 Monte Carlo evaluations.

but it could not treat problems with arbitrarily varying parameters. Of course, neither singular-value approach indicates the likelihood of instability given statistical representatives of parameter variations.

Effects of Actuator Dynamics on Robustness

First-order dynamics for each control are added to the system, which becomes

$$\dot{x}' = F'x' + G'u' \tag{15}$$

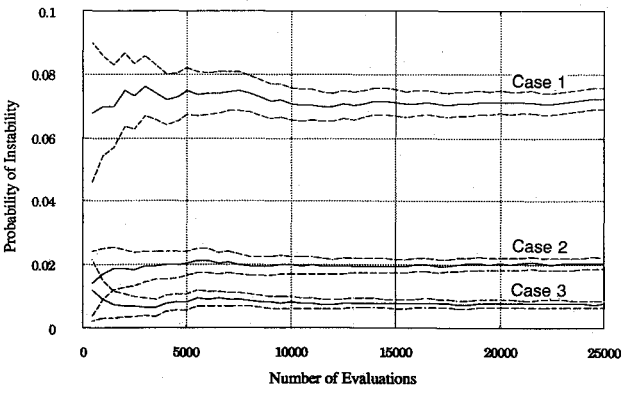

Fig. 3 Ninety-five percent confidence intervals ($\alpha = 0.05$) based on the binomial test for the Forward-Swept-Wing Demonstrator Aircraft with 30% Gaussian parameters and ±30% ρ and V, cases 1, 2, and 3. Probability-of-instability estimates are given by the solid lines. Dashed lines give confidence intervals.

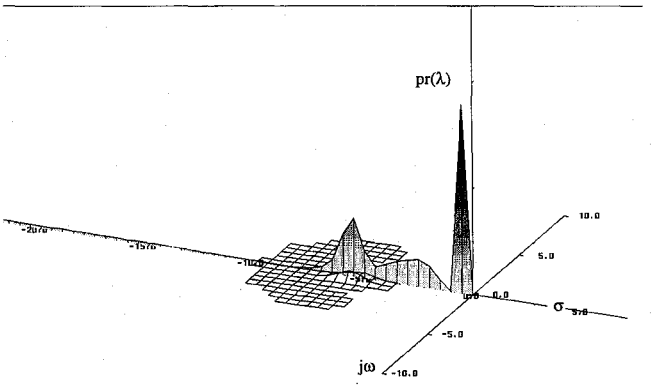

Fig. 4 Stochastic root locus for the Forward-Swept-Wing Demonstrator Aircraft with ±30% uniformly distributed parameters, case 3. Based on 25,000 Monte Carlo evaluations.

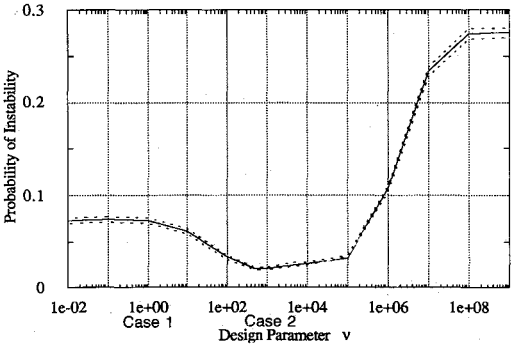

Fig. 5 Probability-of-instability estimates vs control weighting parameter v ($R = vI_2$) for the Forward-Swept-Wing Demonstrator Aircraft. Solid line represents estimate; dashed line represents 95% confidence intervals based on 25,000 evaluations at each of 14 points.

where

$$F' = \begin{bmatrix} & F & & & G & \\ 0 & 0 & 0 & 0 & -\frac{1}{\tau_c} & 0 \\ 0 & 0 & 0 & 0 & 0 & -\frac{1}{\tau_t} \end{bmatrix} \tag{16}$$

$$G' = \begin{bmatrix} 0 & 0 \\ 0 & 0 \\ 0 & 0 \\ 0 & 0 \\ 1 & 0 \\ 0 & 1 \end{bmatrix} \tag{17}$$

The two controls augment the state, and the actuator time constants are included in the subsequent 14-parameter vector:

$$p' = [\rho V f_{11} f_{12} f_{13} f_{22} f_{32} f_{33} g_{11} g_{12} g_{31} g_{32} \tau_c \tau_t]^T \tag{18}$$

Here τ_c is the canard time constant, and τ_t is the thrust setting time constant, whose nominal values are chosen as $\tau_c = 0.1$ s and $\tau_t = 1.0$ s.

A linear-quadratic optimal controller was designed for the new system according to the specification $Q = \text{diag}(1,1,1,0,1,1)$ and $R = \text{diag}(0.001,0.001)$. The intent of these weighting specifications is to approximate as well as possible the controller of case 1, while not pushing the actuator dynamics to unrealistic frequencies. The closed-loop eigenvalues (Table 4) corresponding to the original state are similar to those of case 1, and the eigenvalues associated with actuator dynamics appear as a complex pair. Again, the high-gain controller is purposely chosen to illustrate principles of stochastic robustness.

Stochastic robustness is applied for different values of the variance associated with each time constant, to detail the separate effects of each control lag. Figures 6a–6d show the stochastic root loci, and Table 5 summarizes the probability of instability for each run. The stochastic root loci show that a strong coupling due to uncertainties can occur between the dynamic and control state elements, which tends to push more eigenvalues into the right-half plane. The first and last lines of Table 5 indicate that simply including actuator dynamics increases the probability of instability significantly, even if the associated parameters are known perfectly. This is a reasonable result because actuator dynamics are no longer assumed to be infinitely fast but are allowed to interact with the rigid-body state elements. Qualitatively, bringing actuator-dynamic poles in from infinity pushes the root-locus closer to instability. Stochastic robustness quantifies the effect by showing an increase in the probability of instability estimate of about 2.3%.

The probability of instability for 30% Gaussian parameters and ±30% uniform ρ and V (Fig. 6b) gives a probability-of-instability estimate of 0.09816, for 25,000 cases. Figure 6b shows that the complex pair of eigenvalues has a small variance in the σ direction and a large variance in the $j\omega_d$ direction. The σ-direction variance is largely due to the uncertainty associated with the thrust time constant, as illustrated by increasing the standard deviation on this parameter to 150% in Fig. 6c. Increasing the uncertainty of τ_t has litle effect on the probability of instability because it does not cause further significant coupling with the dynamic modes. Coupling of controller and dynamic modes is largely due to variation of the canard time constant (Fig. 6d). Uncertainty in τ_c causes eigenvalues to migrate to the real axis and split off to form the complex clouds of eigenvalues that reach instability.

Table 4 Parameters for the Forward-Swept-Wing Demonstrator Aircraft with actuator dynamics, case 1

$Q = \text{diag}(1,1,1,0,1,1)$ $R = \text{diag}(0.001,0.001)$

$\lambda_{1\text{-}6} = -33.2,\ -5.14,\ -3.31,\ -0.018,\ -28.35 \pm 17.41j$

$$C = \begin{bmatrix} 5.788 & 4756 & 1209 & 5.539 & 29.78 & -0.6617 \\ 31.04 & -447.0 & -117 & -59.01 & -0.6617 & 55.746 \end{bmatrix}$$

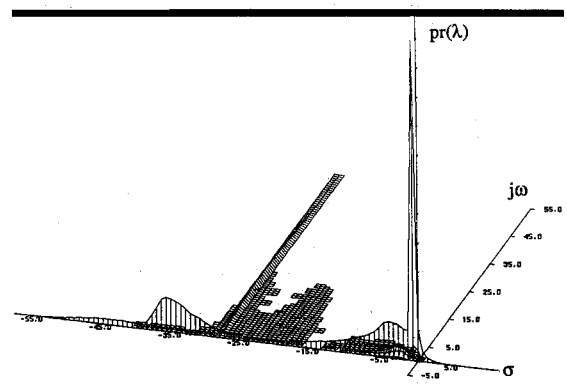

a) Standard deviation of $\tau_c = 0\%$, standard deviation of $\tau_t = 0\%$

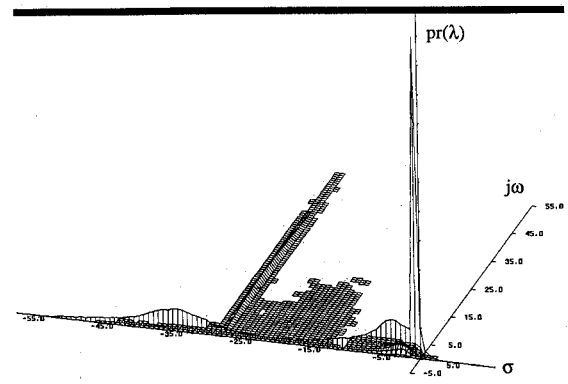

b) Standard deviation of $\tau_c = 30\%$, standard deviation of $\tau_t = 30\%$

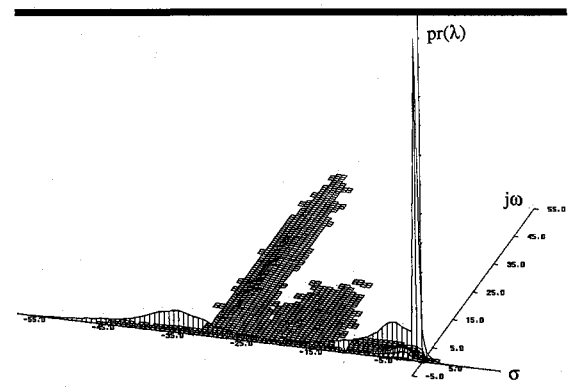

c) Standard deviation of $\tau_c = 30\%$, standard deviation of $\tau_t = 150\%$

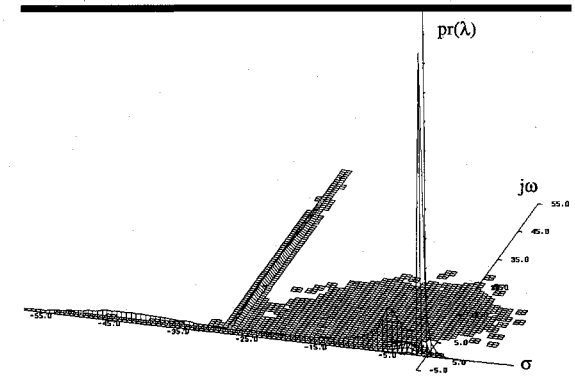

d) Standard deviation of $\tau_c = 150\%$, standard deviation of $\tau_t = 30\%$

Fig. 6 Stochastic root loci for the Forward-Swept-Wing Demonstrator Aircraft with actuator dynamics, for various Gaussian variations of parameters τ_c and τ_t. V, ρ are ±30% uniform, and the remaining parameters are 30% Gaussian. Based on 25,000 Monte Carlo evaluations.

Table 5 Probability of instability for the Forward-Swept-Wing Demonstrator Aircraft with first-order control dynamics for different Gaussian control parameter uncertainties, ±30% uniform V, ρ, and all other parameters 30% Gaussian[a]

Standard deviation of τ_c	Standard deviation of τ_t	$\hat{P}$	95% confidence intervals (L, U)
0	0	0.09572	0.09207, 0.09937
30	30	0.09816	0.09447, 0.10185
30	150	0.09852	0.09483, 0.10221
150	30	0.14316	0.13882, 0.14750
No control dynamics	(Fig. 2a)	0.0724	0.06899, 0.07541

[a]Based on 25,000 Monte Carlo evaluations.

Effects of Higher Order Dynamics on Robustness

With second-order, dynamic-pressure-dependent aeroelastic effects representing the wing's first bending and torsional modes, the (8×8) and (8×2) system matrices can be partitioned as in Ref. 13:

$$F' = \begin{bmatrix} F_r & F_{ra} \\ F_{ar} & F_a \end{bmatrix} \tag{19}$$

$$G' = \begin{bmatrix} G_r \\ G_a \end{bmatrix} \tag{20}$$

where $F_r = F$ and $G_r = G$ represent dynamic and control effects for rigid-body modes given in Eqs. (10) and (11), F_{ra} and F_{ar} couple the rigid and flexible modes, and F_a, G_a represent aeroelastic dynamic and control effects. The appended elements η_b, $\dot{\eta}_b$, η_t, and $\dot{\eta}_t$ represent the first bending mode angle and rate and the first torsional mode angle and rate. In terms of dimensional derivatives, the aeroelastic dynamics are

$$F_a = \begin{bmatrix} 0 & 1 & 0 & 0 \\ \dfrac{(S^1_{\eta_b} - K_b)}{M_b} & \dfrac{S^1_{\dot{\eta}_b}}{M_b} & \dfrac{S^1_{\eta_t}}{M_b} & \dfrac{S^1_{\dot{\eta}_t}}{M_b} \\ \dfrac{S^2_{\eta_b}}{M_t} & \dfrac{S^2_{\dot{\eta}_b}}{M_t} & \dfrac{(S^2_{\eta_t} - K_t)}{M_t} & \dfrac{S^2_{\dot{\eta}_t}}{M_t} \end{bmatrix} \tag{21}$$

$$G_a = \begin{bmatrix} 0 & 0 \\ S^1_{\delta_c} & 0 \\ 0 & 0 \\ S^2_{\delta_c} & 0 \end{bmatrix} \tag{22}$$

where $S^i_{\eta_b}$, $S^i_{\dot{\eta}_b}$, $S^i_{\eta_t}$, $S^i_{\dot{\eta}_t}$, and $S^i_{\delta_c}$ represent structural dimensional derivatives associated with bending and torsional terms; $K_b = 67{,}680$ lb/ft, $M_b = 14$ slugs, $K_t = 5.12E6$ lb/ft, and $M_t = 113$ slugs are the generalized stiffness and mass associated with each mode. The natural frequencies and damping of each mode are functions of stiffness, mass, and aerodynamic terms. Numerical values for F_a and G_a (Table 6) show that the bending mode eigenvalues are strong functions of velocity whereas torsional parameters are largely functions of the generalized mass and stiffness.

The aeroelastic system and coupling matrices introduce an additional 32 nonzero parameters into the system, and a 44-element parameter vector can be assembled, including separate ρ and V effects. While the entire parameter vector could be used for analysis, the parameter vector is reduced to consider just the effects of uncertain coupling terms on robustness. For this example, it is assumed that the dynamics due to material properties and mass of the wing are well known or can be modeled accurately compared to the structural dimensional

Table 6 Numerical values of aeroelastic system matrices and eigenvalues

$$F_{ra} = \begin{bmatrix} 0 & 0 & 0 & 0 \\ -0.32 & -8895 & -2.692 & 0 \\ 0 & 0 & 0 & 0 \\ -2.43E\text{-}3 & 37.44 & -0.2253 & 0 \end{bmatrix}$$

$$F_{ar} = \begin{bmatrix} 0.016 & -1.67E\text{-}4 & -0.297 & 1.13E\text{-}7 \\ 0.0232 & -2.39E\text{-}4 & -0.4435 & 1.71E\text{-}7 \\ 0.145 & 3.41E\text{-}4 & -1.808 & 3.41E\text{-}4 \\ 0 & 0 & 0 & 0 \end{bmatrix}$$

$$F_a = \begin{bmatrix} 0 & 1 & 0 & 0 \\ -1039 & -6.092 & -8139 & -5.12E\text{-}3 \\ 0 & 0 & 0 & 1 \\ -0.2446 & -8.0E\text{-}4 & -45162 & -0.151 \end{bmatrix}$$

$$G_a = \begin{bmatrix} 0 & 0 \\ 170.58 & 0 \\ 0 & 0 \\ 17.058 & 0 \end{bmatrix}$$

$\lambda_{F_a} = -3.05 \pm 32.1j,\ -0.08 \pm 212.5j$

$\lambda_{F'}$ [Eq. (19)] $= -2.95 \pm 32.03j,\ -0.075 \pm 212.5j,$
$-5.12,\ 3.12,\ -0.01 \pm 0.06j$

derivatives appearing in F_{ar}, F_{ra}, F_a, and G_a. The K_b, M_b, K_t, and M_t are assumed to be known perfectly for this analysis. Of the remaining parameters, 16 are chosen for stochastic robustness analysis. These include ρ, V, and the two important rigid-body parameters from the original parameter vector. The remaining parameters are taken from the aeroelastic and coupling matrices:

$$p' = [\rho V f_{32}\ g_{31} f_{61} f_{62} f_{63} f_{65} f_{66} f_{67} f_{82} f_{83} f_{85} f_{88}\ g_{61}\ g_{81}]^T \tag{23}$$

where f_{ij} and g_{ij} represent the elements of the full dynamic and control-effect matrices with velocity and density factored. Table 7 gives the full system matrices in terms of the parameters. For the full-order, open-loop system described by Eq. (19), the eigenvalues associated with bending, torsion, and the original rigid-body modes are

$$\lambda_{1\text{-}8} = -2.95 \pm 32.03j,\ -0.075 \pm 212.5j$$
$$-5.12, 3.12\ -0.01 \pm 0.06j \tag{24}$$

The addition of aeroelastic effects causes a small shift in the original rigid-body eigenvalues.

Evaluation of the three controllers proceeds by applying the reduced-order controller with zeros appended to the full-order system. The controller

$$C' = [C \quad 0] \tag{25}$$

is applied to the full-order system, where C represents the original set of control gains, and 0 is a (2×4) matrix of zeros. Applying this set of gains to the full-order system gives a closed-loop dynamic matrix:

$$F_{cl} = \begin{bmatrix} F_r - G_r C & F_{ra} \\ F_{ar} - G_a C & F_a \end{bmatrix} \tag{26}$$

Equation (26) shows qualitatively that the effect of uncertainty in the coupling terms is magnified through feedback. Table 8

Table 7 Full dynamic matrices as functions of parameters for Forward-Swept-Wing Demonstrator Aircraft with higher order dynamics

$$F = \begin{bmatrix} \frac{-2gf_{11}}{V} & \frac{\rho V^2 f_{12}}{2} & \rho V f_{13} & -g \\ \frac{-45}{V^2} & \frac{\rho V f_{22}}{2} & 1 & 0 \\ 0 & \frac{\rho V^2 f_{32}}{2} & \rho V f_{33} & 0 \\ 0 & 0 & 1 & 0 \end{bmatrix}$$

$$F_{ra} = \frac{\rho V^2}{2} \begin{bmatrix} f_{15} & f_{16} & f_{17} & f_{18} \\ f_{25} & f_{26} & f_{27} & f_{28} \\ f_{35} & f_{36} & f_{37} & f_{38} \\ 0 & 0 & 0 & 0 \end{bmatrix}$$

$$F_{ar} = \begin{bmatrix} 0 & 0 & 0 & 0 \\ \frac{\rho V f_{61}}{M_b} & \frac{\rho V^2 f_{62}}{2M_b} & \frac{\rho V f_{63}}{M_b} & 0 \\ 0 & 0 & 0 & 0 \\ \frac{\rho V f_{81}}{M_t} & \frac{\rho V^2 f_{82}}{2M_t} & \frac{\rho V f_{83}}{M_t} & 0 \end{bmatrix}$$

$$F_a = \begin{bmatrix} 0 & 1 & 0 & 0 \\ \frac{\rho V^2 f_{65}}{2M_b} - \frac{K_b}{M_b} & \frac{\rho V^2 f_{66}}{2M_b} & \frac{\rho V^2 f_{67}}{2M_b} & \frac{\rho V^2 f_{68}}{2M_b} \\ 0 & 0 & 0 & 1 \\ \frac{\rho V^2 f_{85}}{2M_t} & \frac{\rho V^2 f_{86}}{2M_t} & \frac{\rho V^2 f_{87}}{2M_t} - \frac{K_t}{M_t} & \frac{\rho V^2 f_{88}}{2M_t} \end{bmatrix}$$

$$G = \frac{\rho V^2}{2} \begin{bmatrix} g_{11} & g_{12} \\ 0 & 0 \\ g_{31} & g_{32} \\ 0 & 0 \end{bmatrix} \qquad G_a = \frac{\rho V^2}{2} \begin{bmatrix} 0 & 0 \\ g_{61} & 0 \\ 0 & 0 \\ g_{81} & 0 \end{bmatrix}$$

Table 8 Closed-loop eigenvalues for reduced-order (fourth-order) controllers applied to eighth-order Forward-Swept-Wing Demonstrator Aircraft model

Case 1	Bending mode:	$-2.29 \pm 32.0j$
	Torsion mode:	$-0.097 \pm 212.5j$
	Rigid body:	$-4.96 \pm 1.27j$, -35, -0.019
Case 2	Bending mode:	$-2.53 \pm 32.0j$
	Torsion mode:	$-0.089 \pm 212.5j$
	Rigid body:	$-4.8 \pm 1.38j$, -1.01, -0.022
Case 3	Bending mode:	$-1.75 \pm 32.88j$
	Torsion mode:	$-0.144 \pm 212.5j$
	Rigid body:	-3.6, -5.51, -34.1, -0.021

quantifies the effect on the nominal system by presenting the eigenvalues of the closed-loop system for each controller. The closed-loop mean eigenvalues of rigid-body modes shift from the reduced-order case because of the presence of the added dynamics. In each case, the open-loop bending mode eigenvalues ($-2.95 \pm 32.03j$) shift toward instability.

Next, stochastic robustness analysis is applied to the full-order system. Figure 7 shows the stochastic root locus for $\pm 30\%$ uniform variations in velocity and density alone, using the case 2 gains established previously for the reduced-order system. The trend in eigenvalue migration toward instability with ρ and V variations is similar for case 1 and case 3. For 5000 Monte Carlo evaluations, the probabilities of instability

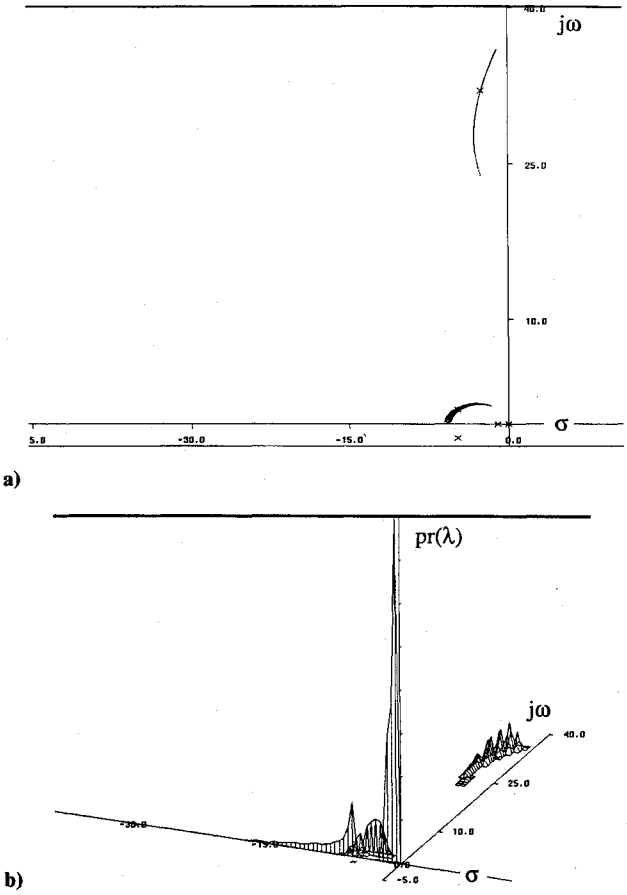

Fig. 7 Stochastic root locus for the Forward-Swept-Wing Demonstrator Aircraft with known rigid-body and aeroelastic parameters, and $\pm 30\%$ uniform V and ρ variations, case 2. Based on 5,000 Monte Carlo evaluations.

are zero. As expected, the closed-loop torsion eigenvalues at $s = -0.1 \pm 212.5j$ (not shown in Fig. 7) do not change significantly with velocity and do not affect the probabilities of instability. Bending mode eigenvalues show a definite velocity trend, migrating towards instability along a curved root locus path as velocity increases. The top view of Fig. 7 is composed of individual Monte Carlo evaluations. Note that binning these along the curved path gives a jagged three-dimensional distribution in Fig. 7b.

Figure 8 shows the stochastic root locus for $\pm 30\%$ uniform variations in ρ and V and 30% Gaussian variations in the remaining 14 parameters, using the case 2 gains. The portion of each stochastic root locus associated with the rigid-body dynamics is similar to its Fig. 2 counterpart. The peak near the origin is magnified to bring out the distribution associated with the bending mode eigenvalues. For each controller, corresponding probability of instability estimates and 95% confidence intervals for 10^5 evaluations are 1) 0.045447 (0.04416, 0.04674), 2) 0.01083 (0.01019, 0.01147), and 3) 0.038667 (0.03747, 0.03987). Figure 9 presents the confidence interval estimates as functions of number of evaluations. By 10^5 evaluations it is evident that the probability-of-instability estimates have settled within very narrow intervals. Although these results cannot be compared directly with the results of Fig. 2 (because of the reduction in the parameter space associated with the reduced-order system), definite trends are evident. The disparity in robustness between cases 1 and 3 is reduced, and case 3 shows a considerable decrease in robustness, while the robustness of the first two cases is at least retained or possibly improved. Application of a reduced-order controller to a higher order system does not guarantee that the robustness margins of the original system are retained, but the robustness of the system does not always decrease. Stochastic

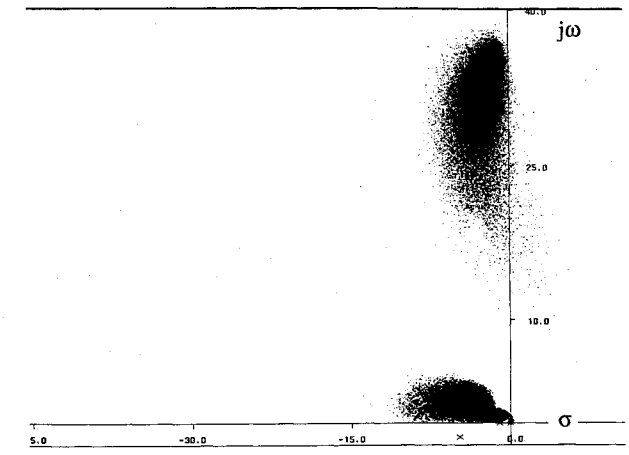

Fig. 8 Stochastic root locus for Forward-Swept-Wing Demonstrator Aircraft with aeroelastic modes, ±30% uniform V and ρ variations, and 30% Gaussian variations in the remaining 14 parameters, case 2. Based on 10^5 Monte Carlo evaluations.

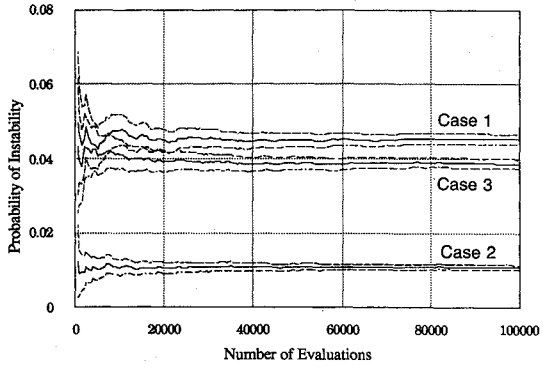

Fig. 9 Confidence intervals (95% or $\alpha = 0.05$) based on the binomial test for the Forward-Swept-Wing Demonstrator Aircraft with aeroelastic modes, cases 1, 2, and 3. Probability-of-instability estimates are given by the solid lines. Dashed lines give confidence intervals.

robustness again provides an excellent framework for quantifying the effects of applying a reduced-order controller to a higher order system.

Conclusion

Stochastic robustness offers a rigorous yet straightforward alternative to current metrics for evaluating the effects of parameter variations on control systems that is simple to compute and is unfettered by normally difficult problem statements, such as non-Gaussian statistics, products of parameter variations, and structured uncertainty. The approach answers the question, How likely is the closed-loop system to fail, given limits of parameter uncertainty? By requiring known or estimated parameter distributions, and using confidence interval calculations, unduly conservative (at the expense of performance) or insufficiently robust control system designs in the face of real-world uncertainties are avoided.

The examples presented here illustrate the use of stochastic robustness and its advantage in studying both full-state and reduced-order aircraft control systems. The parameters of aircraft stability-and-contol-effect matrices (stability derivatives and nominal flight condition parameters) lend themselves to this type of analysis tool. The stochastic robustness estimates of different control system designs can be directly compared. The method can be applied to finite-dimensional model-order uncertainties in aircraft control systems by adding the uncertain dynamics to the system and assigning appropriate statistics to the new parameters. Quantitative effects of individual parameters or combinations of parameters on robustness can be measured in terms of the probability of instability. The principal difficulty in applying this method to control systems is that it is computationally intensive; however, requirements are well within the capabilities of existing computers. The principal advantage of the approach is that it is easily implemented and makes good use of modern computational and graphic tools, and results have direct bearing on engineering objectives.

Acknowledgments

This research has been sponsored by the Federal Aviation Administration and the NASA Langley Research Center under Grant NGL 31-001-252. The authors are grateful to Wallace VanderVelde of MIT for helpful discussions on this subject.

References

[1]Dorato, P. (ed.), *Robust Control,* IEEE Press, New York, 1987.

[2]Stengel, R. F., "Some Effects of Parameter Variations on the Lateral-Directional Stability of Aircraft," *Journal of Guidance and Control,* Vol. 3, No. 2, 1980, pp. 124–131.

[3]Stengel, R. F., *Stochastic Optimal Control: Theory and Application,* Wiley, New York, 1986.

[4]Stengel, R. F., and Ryan, L. E., "Stochastic Robustness of Linear Control Systems," *Proceedings of the 1989 Conference on Information Sciences and Systems,* Johns Hopkins Univ., Baltimore, MD, March 1989, pp. 556–561.

[5]Stengel, R. F., and Ryan, L. E., "Multivariate Histograms for Analysis of Control System Robustness," *Proceedings of the 1989 American Control Conference,* Pittsburgh, PA, June 1989, pp. 937–943.

[6]Stengel, R. F., and Ray, L. R., "Stochastic Robustness of Linear-Time-Invariant Control Systems," *IEEE Transactions on Automatic Control,* Vol. 6, No. 1, pp. 82–87.

[7]Evans, W. R., "Graphical Analysis of Control Systems," *Transactions of the American Institute of Electrical Engineers,* Vol. 67, 1948, pp. 547–551.

[8]Conover, W. J., *Practical Non-Parametric Statistics,* Wiley, New York, 1980.

[9]Sandell, N. R., Jr. (ed.), "Recent Developments in the Robustness Theory of Multivariable Systems," Office of Naval Research, Rept. ONR-CR215-271-1F, Arlington, VA, Aug. 1979.

[10]Doyle, J. C., "Analysis of Feedback Systems with Structured Uncertainties," *IEE Proceedings,* Vol. 129, Pt. D, No. 6, Nov. 1982, pp. 242–250.

[11]Tahk, M., and Speyer, J. L., "Modeling of Parameter Variations and Asymptotic LQG Synthesis," *IEEE Transactions on Automatic Control,* Vol. AC-32, No. 9, Sept. 1987, pp. 793–801.

[12]Morton, B. G., and McAfoos, R. M., "A Mu-Test for Robustness of a Real-Parameter Variation Problem," *Proceedings of the 1985 American Control Conference,* Boston, MA, June 1985, pp. 135–138.

[13]Gilbert, M. G., *Dynamic Modeling and Active Control of Aeroelastic Aircraft,* M.S. Thesis, Purdue University, West Lafayette, IN, 1982.